Electronic Supplementary Material (ESI) for RSC Advances.

"d-Electron interactions" Induced CoV_2O_6-Fe-NF for Efficient Oxygen Evolution Reaction

Yuchao Guo,[a] Gaojie Yan [a], Xi Sun [a], Shuo Wang [a], Li Chen [a], Yi Feng* [a]

[a]Hebei Key Laboratory of Functional Polymers, Department of Polymer Materials and Engineering, Hebei University of Technology, Tianjin 300400, P. R. China.
E-mail: luckyii0512@163.com

Experimental Section

Chemicals：

NH_4VO_3 (99%), $Co(NO_3)_2 \cdot 9H_2O$ (99.99%) and $FeCl_3$ (98%) were purchased from Aladdin Ltd (Shanghai, China). Sodium Lauryl Sulfonate (SLS 98.0%) were purchased from Aladdin Bio-Chem Technology Co., LTD (Shanghai, China). HCl (36 wt%) were supplied by Huanghua SJKB Technology Development Co., Ltd (Hebei, China).

Pretreatment of the *Nickel Foam (NF)*：

The Nickel Foam (NF) was first cut into pieces of size 1 cm × 3 cm. The cut pieces of NF were sonicated in a 1 M HCl solution for 15 minutes to remove the oxide layer on their surface, followed by alternate sonication with distilled water and absolute ethanol to remove any residual HCl. The pieces were immediately dried to prevent their surface from continuing to oxidize.

Synthesis of *CoV_2O_6-NF*：

CoV_2O_6-NF was synthesized using a simple precipitation method. 1.5 mmol of

NH_4VO_3 was dissolved in 50 mL of deionized water (DIW) and stirred at 90°C for 30 minutes to obtain a clear and uniform solution. The NF and 0.15 mmol of SLS were added to the solution. 5 mL of 0.1 M $Co(NO_3)_2 \cdot 9H_2O$ solution was slowly added. The mixture was stirred at 90°C for 60 minutes. After cooling to room temperature, the NF was washed alternately with deionized water and absolute ethanol, and finally vacuum dried at 60 °C overnight.

Synthesis of *Fe-NF*：

1 mmol $FeCl_3$ was dissolved in 50 ml of DIW. The NF was soaked in the solution for 15 minutes to obtain the Fe-NF.

***Synthesis of CoV_2O_6-Fe-NF*：**

CoV_2O_6-Fe-NF was synthesized in a similar manner to CoV_2O_6-NF, except that Fe-NF was used instead of NF.

Characterizations:

The crystal phase of the product was analyzed using X-ray diffraction (XRD) with a D8 Discover instrument operating at 40 kV and 120 mA, and a Cu Ka radiation source. The materials for the XRD test samples were subjected to sonication in ethanol and subsequently vacuum dried at 60 °C. The morphology of the samples was examined using a scanning electron microscope (SEM) with an FEI Nova Nano SEM450 and a transmission electron microscope (TEM) with a JEOL JEM-2100F. The weight ratio of Co, Fe, V, and Ni elements in the sample was determined using inductively coupled plasma optical emission spectroscopy (ICP-OES) with an Agilent 725ES & Agilent 5110. For TEM samples, the materials were sonicated in ethanol and then cast on a carbon-coated copper mesh. The surface characteristics of the samples were studied using an FEI ESCALAB 250Xi X-ray photoelectron spectrometer (XPS), and all XPS

peaks were calibrated using C 1s (284.8 eV). In-situ Raman spectra were recorded using a CCD confocal microprobe Raman system (Renishaw inVia Reflex, British) with a 50× magnification long working distance (8 mm) objective and a 532 nm wavelength excitation laser from a He-Ne laser with a power of approximately 4 mW. The Raman frequencies were calibrated using a Si wafer, and the spectra were collected for 30 seconds with one single spectrum curve, accumulated three times. For in-situ Raman measurements, a custom-made spectroelectrochemical cell with a working electrode (the prepared CoV_2O_6-Fe-NF catalyst), a graphite counter electrode, and a reference electrode (Ag-AgCl) was used with an electrolyte solution made of 1 M KOH.

Electrochemical measurements:

All electrochemical measurements were conducted at room temperature using a CHI760E electrochemical workstation, employing a standard three-electrode configuration. The working electrode consisted of the prepared metal foam materials, while a Hg-HgO (KOH saturated) electrode served as the reference electrode, and platinum was used as the counter electrode. The alkaline environment was created using a 1M KOH electrolyte. To obtain reversible hydrogen electrode (RHE) potentials, iR compensation was applied using the following equation:

$$E_{(RHE)} = E_{(Hg\text{-}HgO)} + 0.059pH + 0.098V \quad (1)$$

Overpotential(η) was determined as follows:

$$\eta = E_{(RHE)} - 1.23V \quad (2)$$

Linear sweep voltammetry (LSV) measurement for evaluating the OER performance was recorded at a scan rate of 2 mV s^{-1} to obtain the polarization curves. Tafel slope was calculated from the linear region -without Faradic current- of the

polarization curve, which could be fitted using the Tafel empirical equation:

$$\eta = a + b\lg J \quad (3)$$

Where J is the current density (mA cm^{-2}), b represented the tafel slope (mV dec^{-1}).

Electrochemical impedance spectroscopy (EIS) was performed at potential of 605 mV (V vs. Hg-HgO) with frequency from 0.01 to 100,000 Hz and an amplitude of 5 mV. The long-term stability test was performed by chronoamperometric electrolysis at 50 mA cm^{-2}. The electrochemical double-layer capacitance was determined from the CV curves measured in a potential range of 0.01 V-0.06 V (vs. Hg-HgO) without redox processes according to the following equation:

$$C_{dl} = \frac{j}{v} \quad (4)$$

where C_{dl}, j, and v are the double-layer capacitance (mF cm^{-2}) of the electroactive materials, charging current (mA cm^{-2}), and scan rate (mV s^{-1}), respectively. The C_{dl} can be further converted into electrochemically active surface area (ECSA) using the follow equation, and the Cs used 40 μF·cm^{-2} [1].

$$ECSA = \frac{C_{dl}}{C_s} \quad (5)$$

The turnover frequency (TOF) values were calculated as the number of oxygen molecules evolved per active site per second based on the following equation[2,3]:

$$TOF = \frac{J \times A}{4 \times F \times m} \quad (6)$$

The current density "J" (A cm^{-2}) at a specific overpotential is calculated using the

effective surface geometric area "A" (1 cm^2) of the working electrode, Faradaic efficiency "F" (96485 s A·mol^{-1}), and the number of moles "m" of the active metal on the electrode, which is determined by the ICP-OES results.

The number of moles (m) is calculated from ICP-OES results:

CoV_2O_6-Fe-NF (active metal is Fe and Co): atomic percentage: Fe 3.41 %, Co 26.78 %, V 69.81%.

Loading of CoV_2O_6-Fe-NF was about 0.73 mg.cm^{-2}. We set total mols of Fe, Co, V, as x, we could get:

$55.85*0.0341\ X + 58.93*0.2678X + 50.94*0.6981X = 0.73*10^{-3}$

$m = (0.0341+0.2678)\ X = 4.199*10^{-6}$ g

CoV_2O_6-NF (active metal is Co): atomic percentage Co 27.72%, V 62.28% Loading of CoV_2O_6-NF was about 1.09 mg.cm^{-2}

Similarly, $58.93*0.2772X + 50.94*0.6228X = 1.09*10^{-3}$

$m = 0.2772X = 6.287*10^{-6}$ g

Supplemental Figures and Tables

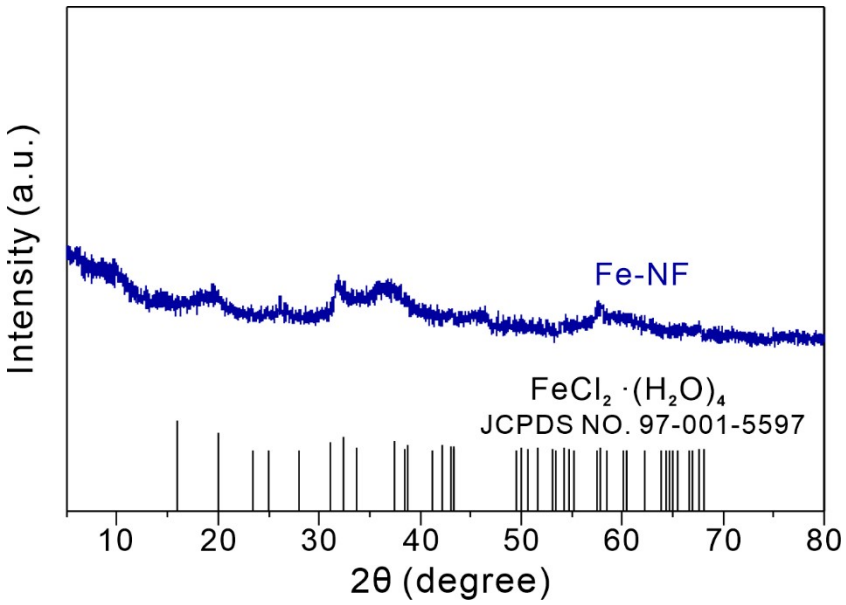

Fig. S1 XRD patterns of Fe-NF.

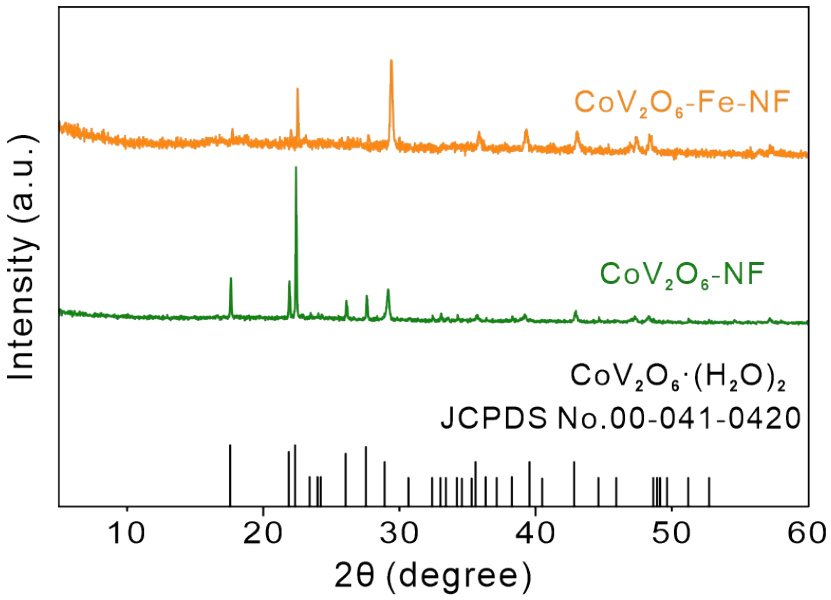

Fig. S2 XRD patterns of CoV_2O_6-NF and CoV_2O_6-Fe-NF.

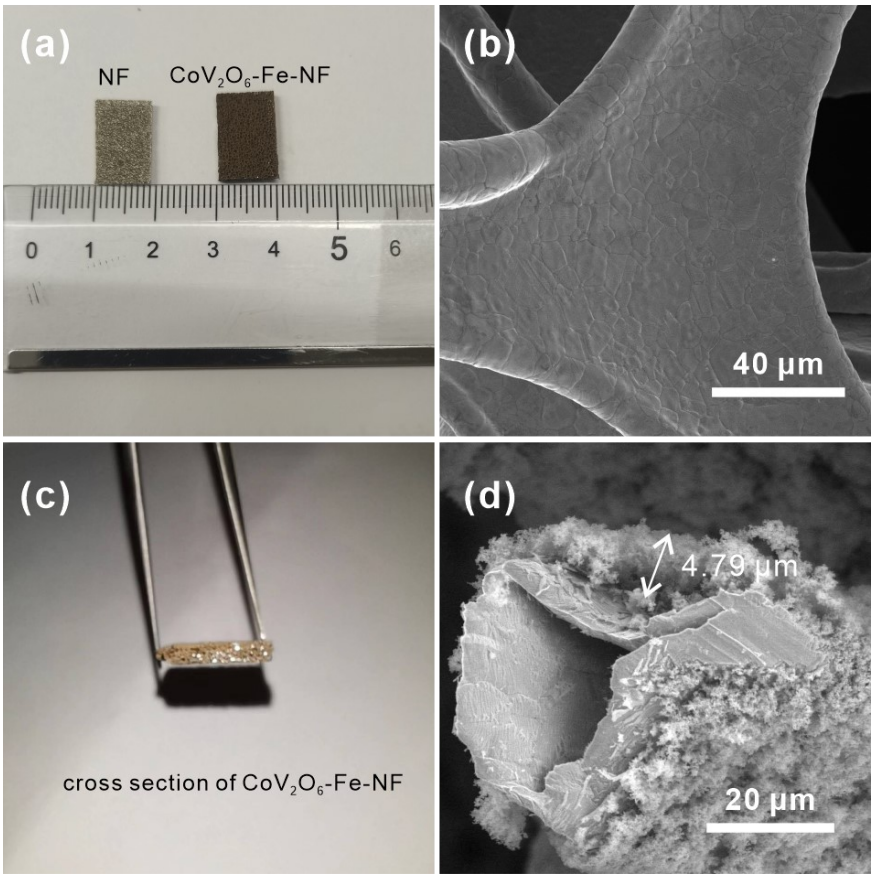

Fig. S3 (a) physical photo of NF and CoV_2O_6-Fe-NF, (b) SEM image of NF, (c) physical photo of the cross section of CoV_2O_6-Fe-NF, (d) SEM image of the cross section of CoV_2O_6-Fe-NF

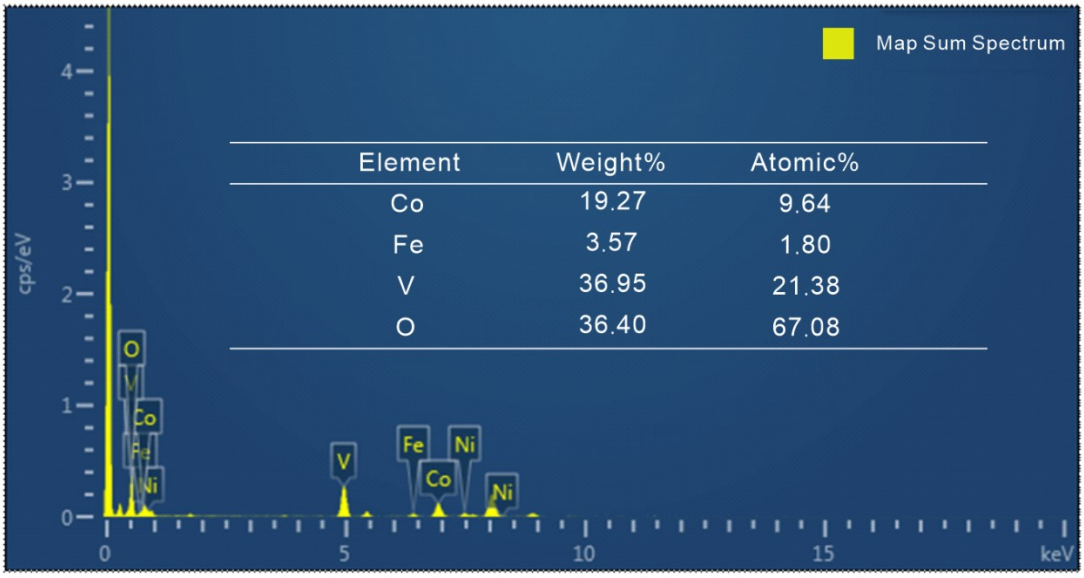

Fig. S4 EDS of the CoV_2O_6-Fe-NF; Inset is the corresponding weight and atomic ratio of Co, Fe, Ni, V, and O elements.

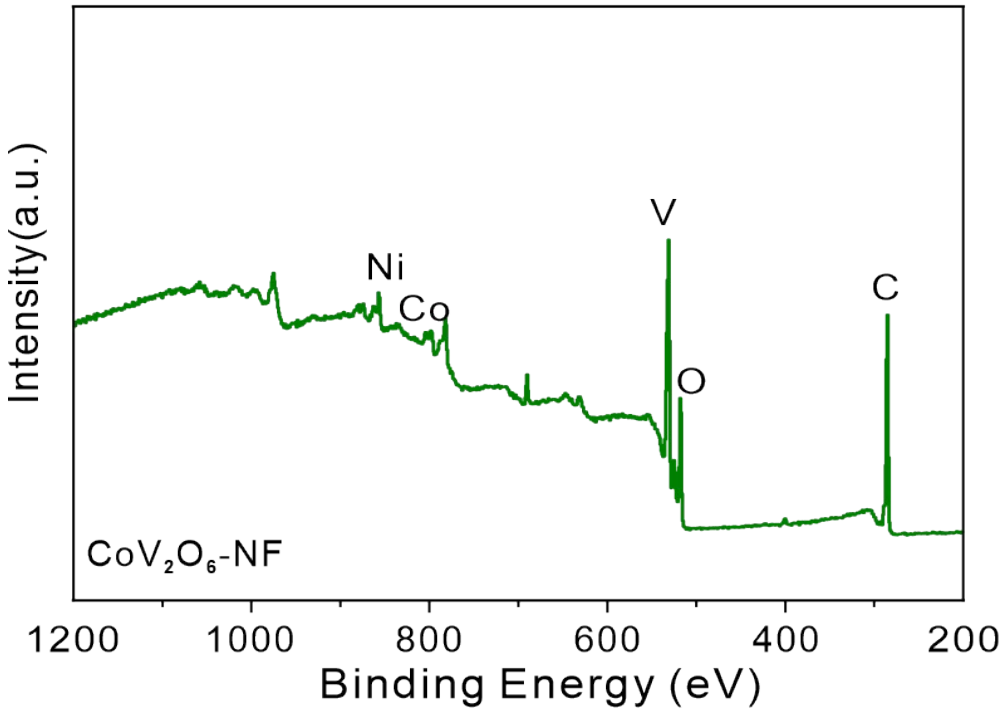

Fig. S5 XPS survey of CoV_2O_6-NF.

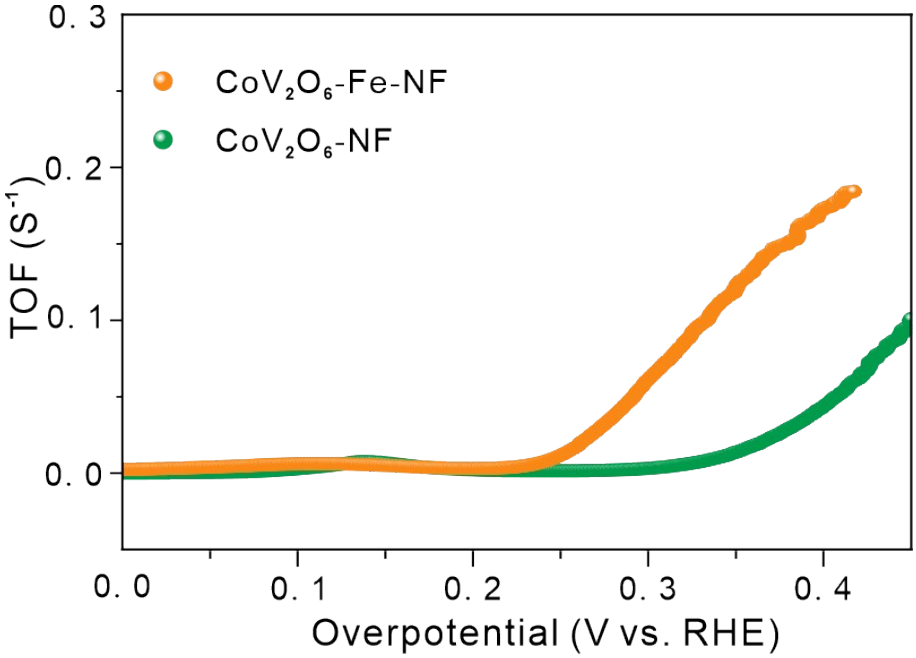

Fig. S6 TOF plots of CoV_2O_6-Fe-NF and CoV_2O_6-NF

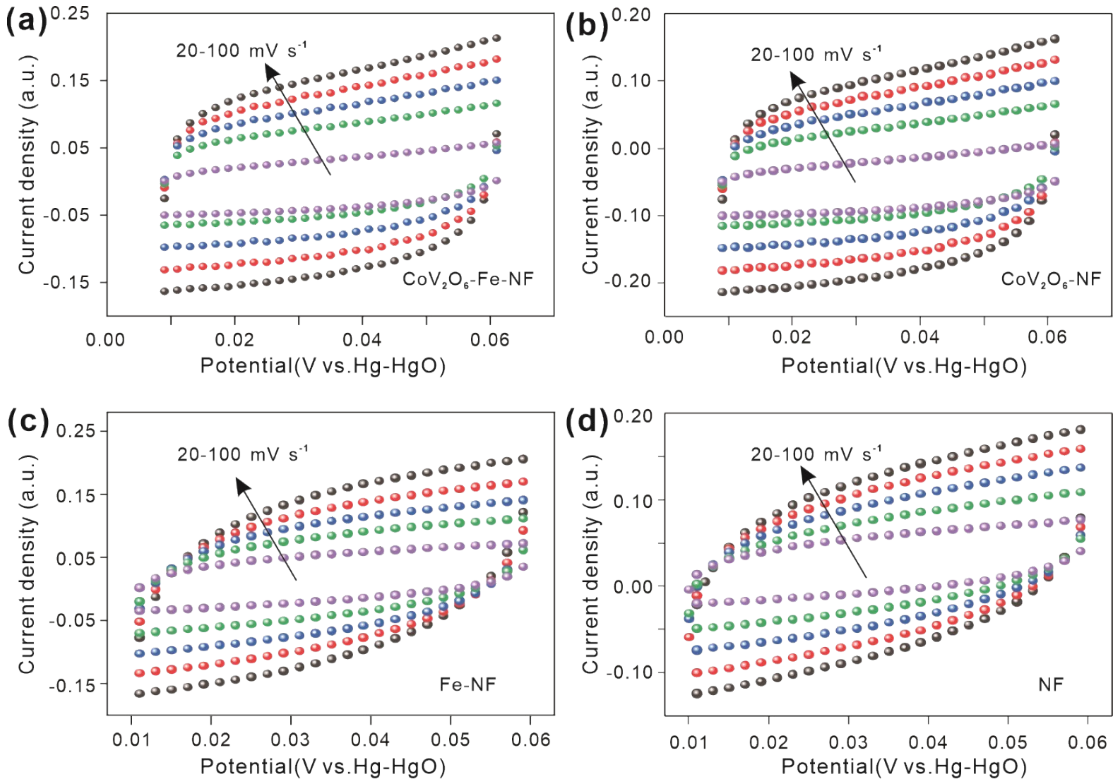

Fig. S7 OER Electrochemical capacitance of (a) CoV_2O_6-Fe-NF, (b) CoV_2O_6 -NF, (c) Fe-NF and (d) NF measured in the non-Faradaic potential range (0.01-0.06 V vs. Hg-HgO) at scan rates of 20, 40, 60, 80, 100mV s^{-1}.

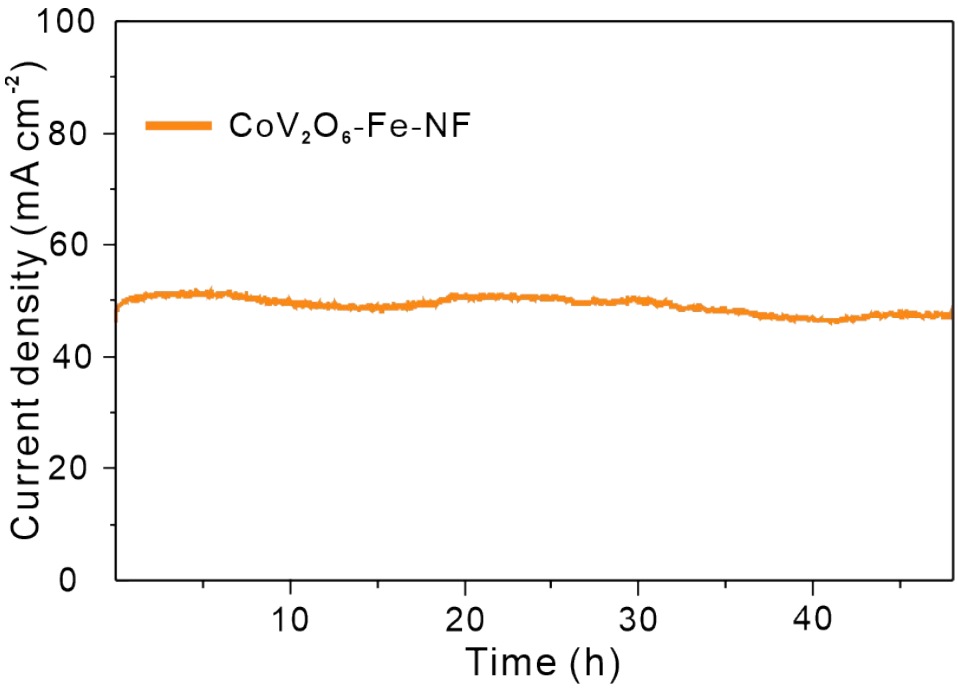

Fig. S8 Stability curve of CoV_2O_6-Fe-NF.

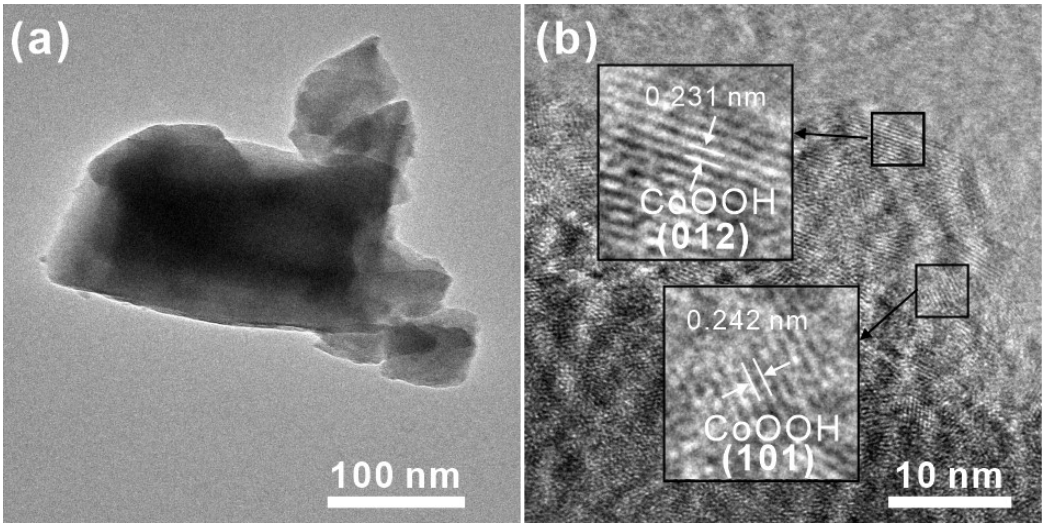

Fig. S9 (a)TEM, and (b) HRTEM image of post-OER CoV_2O_6-NF

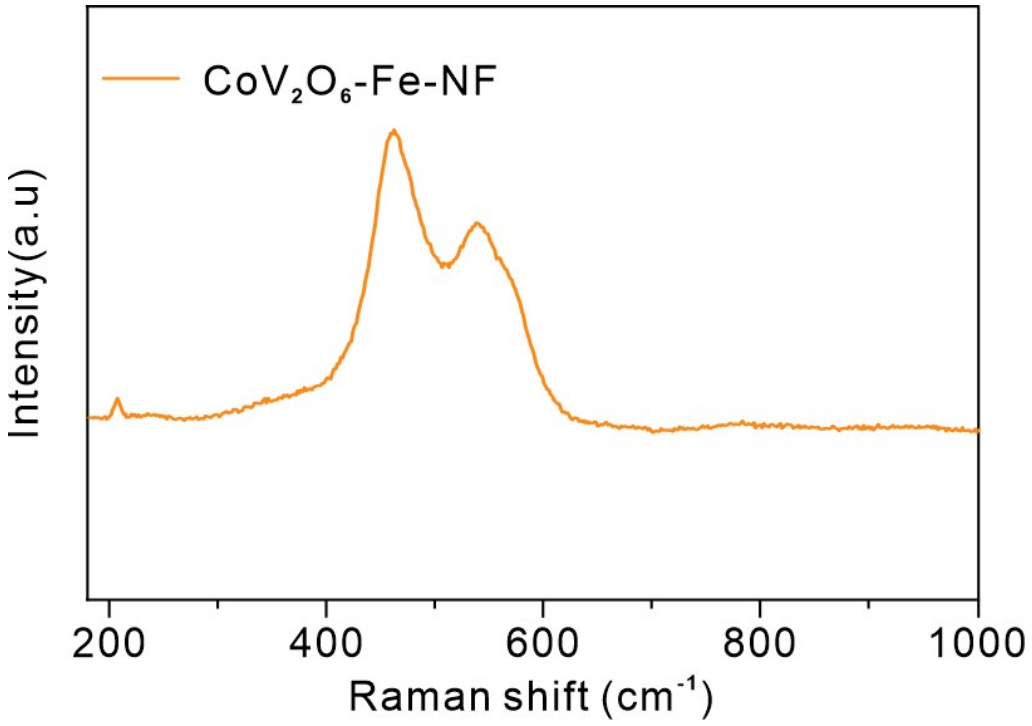

Fig. S10 Raman spectra of post-OER CoV_2O_6-Fe-NF

Table S1 ICP-OES analysis data for the weight and atomic ratios of metals of the prepared CoV_2O_6-Fe-NF

Sampling quality/g	Element	Weight%	Atomic%
0.0428	Co	31.54	28.51
0.0428	Fe	4.11	3.92
0.0428	V	64.45	67.57

Table S2 Co and V XPS fitting parameters of binding energies and peak area ratio for the catalyst.

Catalyst	Binding energy (eV)				Co^{3+}/Co^{2+}	Binding energy (eV)				V^{5+}/V^{4+}
	Co^{3+}		Co^{2+}			V^{5+}		V^{4+}		
	$2p_{3/2}$	$2p_{1/2}$	$2p_{3/2}$	$2p_{1/2}$		$2p_{3/2}$	$2p_{1/2}$	$2p_{3/2}$	$2p_{1/2}$	
CoV_2O_6-NF	780.85	796.90	782.70	798.55	0.88	517.37	524.76	517.02	523.78	0.82
CoV_2O_6-Fe-NF	780.62	796.53	782.26	797.69	0.66	517.32	524.75	516.96	523.77	0.65

Table S3. ICP-OES analysis data for the weight and atomic ratios of metals of the prepared Fe-NF（None ultrasonic treatment）

Sampling quality/g	Element	Weight%	Atomic%
0.0788	Ni	93.62	93.29
0.0788	Fe	6.38	6.71

Supplementary references

1 R. Zhang, Z. Wei, G. Ye, G. Chen, J. Miao, X. Zhou, X. Zhu, X. Cao and X. Sun, "d-Electron Complementation" induced V-Co phosphide for efficient overall water splitting, Adv. Energy Mater., 2021, 11, 2101758. https://doi.org/10.1002/aenm.202101758

2 W. Wang, Y. Zhang, X. Huang and Y. Bi, Engineering the surface atomic structure of $FeVO_4$ nanocrystals for use as highly active and stable electrocatalysts for oxygen evolution, *J. Mater. Chem. A*, 2019, **7**, 10949-10953. https://doi.org/10.1039/C9TA02922B

3 F. Song, M. M. Busch, B. L. Kasier, C. S. Hsu, E. Petkucheva, M. Bensimon, H. M. Chen, C. Corminboeuf and X. Hu, An unconventional iron nickel catalyst for the oxygen evolution reaction, *ACS Cent. Sci.,* 2019, **5**, 558-568. https://doi.org/10.1021/acscentsci.9b00053